Progress In Electromagnetics Research C, Vol. 127, 195–205, 2022

3D Printed Low Profile Strip-Based Helical Antenna

Purno Ghosh* **and Frances J. Harackiewicz**

Abstract—A copper strip and conductive paint-based low profile stripped helical antenna for circular polarization over wide axial-ratio (AR) bandwidth are presented. Impacts of strip widths and geometric parameters of the helix on antenna performance (impedance bandwidth, reflection coefficient, AR, gain) are analyzed thoroughly. In terms of performance parameters, the proposed design is also compared with traditional designs of wire and strip-based helical antennas. Proper impedance matching in the proposed design is achieved by the non-conformal placement of the strip. For easing the fabrication complexity, the antenna is again simulated with a dielectric-based supportive structure, and the impact of this additional support is discussed. The antenna is then constructed on a 3D printed polylactic acid (PLA) based structure. Finally, the 1.3-turn strip-based helical antenna with a radius of 18 mm provided impedance and 3-dB AR bandwidths of 99% and 82.52%, respectively. The maximum gain of 9.40 dBi was found at 2.05 GHz in 3-dB AR bandwidth. The height of the presented antenna is 0.35 λ_0, where λ_0 is the free space wavelength at the frequency of 2.65 GHz. Low profile and wide AR bandwidth facilitate the use of this antenna in space communication.

1. INTRODUCTION

A helical antenna is an excellent candidate for producing circular polarization (CP). Traditional wire-based helical antennas are still serving this purpose effectively. But due to the large height in the axial direction, this antenna does not satisfy the requirement where size and spaces are issues. Although some of the low-profile helical antennas have been reported in [1, 2], the AR bandwidth is around 12%. Beyond the cylindrical helix, Hui et al. [3] proposed a low-profile hemispherical helix with maximum AR bandwidth of 14.6% but covers a wide angular range. Another tapered metallic strip-based compact hemispherical helix presented in [4] provides improved AR bandwidth of 24% but requires an additional wire segment for impedance matching. A very low-profile end fire planar helical antenna with 34% of AR bandwidth is reported in [5]. The quadrifilar helical antennas constructed on a poly-amide substrate and PLA substrate are reported in [6, 7]. Besides the helical antenna, a dipole antenna is also constructed using wood-based PLA and silver nano-particle ink [8]. Compared to the above traditional wire and print-based planar helical antennas, constant width strip-based cylindrical helix antenna is something new. A 1.1-turn strip helical antenna with an antenna height of $0.52\lambda_0$ presented in [9] provides an AR bandwidth of 46%, and the conductive strip face is normal to the ground plane. That perpendicular placement does not always ensure a proper impedance matching without an extra matching section. Authors in [10] also studied strip-based helical antennas and kept the orientation of the strip face parallel to the ground plane for ensuring the impedance matching issue. The radius of the helix was 30 mm, and they found the CP radiation when the number of helical turns was at least 2.5. AR bandwidth of 17% was achieved for an antenna height of 41 mm without using the parasitic patch, although 44% AR bandwidth was obtained by adding a parasitic patch at the top of the helix. Strip

Received 15 October 2022, Accepted 14 December 2022, Scheduled 16 December 2022
* Corresponding author: Purno Ghosh (purno.ghosh@siu.edu).
The authors are with the School of Electrical, Computer and Biomedical Engineering, Southern Illinois University Carbondale, IL, USA.

helix arms printed on four individual rectangular-shaped FR4 substrate materials and then combined to form a final rectangular-shaped end fire helix are presented in [11], and the AR bandwidth of 54% is achieved with an antenna height of 155 mm. A review article [12] focuses on the advantage of additive manufacturing in the design of antennas and RF structures. A wide variety of antennas were cited, which were fabricated using modern 3D printing technology.

A 3D printed spiral wire-like helical antenna with nickel and copper electroless plating is shown in [13] where a printed quarter wave transformer is used for impedance matching. In [14–16], a wire helix, a tapered helical antenna, and a horn antenna are constructed using inkjet and 3d printers, respectively. The impacts of 3D printing on the radiation characteristics of dielectric lens antenna are analyzed in [17]. Measurement of electrical parameters of PLA material and thereby construction of three antennas have been presented in [18].

It is not straightforward to construct any non-planar helical antenna by maintaining the proper alignment of conductive elements and desired spacing among turns. If it is a strip form, then the challenge is more arduous, and it may be one of the reasons that there are very few works on strip helix with durable fabrication. In [9], after rolling the substrate material manually, it may not be a perfect cylindrical shape because the thickness as mentioned there is only 0.5 mm. Even making sure the smooth connection between two long ends of the substrate material is another matter of concern because the number of turns is more than one that crosses the intersection. Foam has been used in [10] for supporting the structure, and it is nondurable and temporary. According to the picture of constructed antenna, there is a very chance of deviation of the strip conductor due to handling and tilting the whole antenna system. Similarly, joining strips printed on four rectangular materials may cause any misalignment, and combining with the ground plane is an issue that needs extra consideration [11].

In our work, four things are focused on before starting the analysis: keeping the number of helical turns and height of the antenna in the axial direction as low as possible, circular polarization over a wide bandwidth, the optimum gain under 3-dB AR bandwidth, and finally and the most importantly a stable and rapid method of construction of a strip-based helical antenna. Impedance, AR, gain, and radiation patterns are observed in detail through simulation by varying different geometric parameters of the helix. The impacts of dielectric support on antenna performance parameters are also investigated. Simulation analysis is carried out using CST microwave studio. 3D printer (Sindoh 3D WOX) is used for printing the PLA-based supportive structure and then constructing the antenna using copper tape and conductive paint as two independent approaches. Detailed construction procedures and measurement of the above antenna parameters are discussed later in the corresponding measurement section.

2. GEOMETRY OF THE STRIP-BASED ANTENNA

The geometry of the proposed strip-based helical antenna is shown in Fig. 1. The helical arm is rotated in the counterclockwise direction for righthand circular polarization. Parameters such as the radius of the helix (R), number of turns (N), spacing between turns (S), pitch angle (α), and diameter of the ground plane (D) describe the complete geometry of the helical antenna. Because of the strip form, an extra parameter 'W' for the width of the strip is introduced. The radius (R) of the helix is chosen as 18 mm which gives the circumference (C) of 113 mm and is also equivalent to one wavelength at 2.65 GHz. The proposed helix maintained a constant pitch angle (α) of 14°, and the spacing (S)

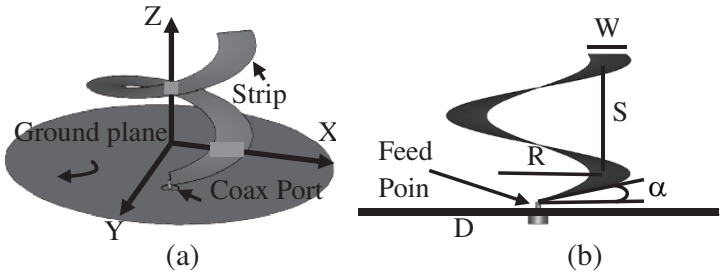

Figure 1. Configuration of strip-based helical antenna: (a) 3D view, (b) front view.

between turns is kept at 28.18 mm ($S = C\tan\alpha$) which is about one-quarter of the wavelength. The diameter (D) of the circular-shaped flat ground plane is 135 mm which is more than one wavelength. The gap between the bottom end of the strip helix (feed end) and the ground plane is 3.20 mm. The height of the proposed 1.3 turns strip helix is 36.64 mm, and considering the feeding gap, the total height is 39.84 mm which is equivalent to $0.35\lambda_0$, where λ_0 is the free space wavelength at the frequency of 2.65 GHz.

3. ANALYSIS AND SIMULATION RESULTS

The helical antenna operates in two modes, namely normal mode and axial mode. In this communication, the axial mode helix is considered, where the intensity of maximum radiation from the antenna will be concentrated in a major lobe, and the alignment of this lobe will be along the height of the helix. To operate at this axial mode, the radius of the helix, spacing between turns, pitch angles, and size of the ground plane follow certain design requirements [19]. By following the design requirement of the wire-based helix, a strip-based helix is designed which replace the circular wire with a flat conductor of constant width. For strip-based arrangement, wide circular polarization bandwidth can be achieved when the forward current at the end of the strip maintains values greater than zero, which overall minimizes the reflected current along the strip length [10]. Corresponding values of the helix parameters are provided in the above section.

3.1. Simulation without Supportive Structure

The simulated wire and strip-based helical antenna structures with two different orientations of the strip are shown in Fig. 2. Simulation is carried out to explain the effects of orientation of the strip, strip widths (W), number of turns (N), and pitch angles (α) on reflection coefficient (S_{11}), 3-dB AR bandwidth, and gain of the strip-based helical antenna. The 'strip orientation' means the placement of the face of the spiral conducting strip concerning the ground plane. For example, vertical (ver.) is used when the wide face of the strip is perpendicular to the circular face of the ground plane. The parameters W, N, and α vary throughout the analysis. The change in operation frequency with the radius (R) [10] of the helix is not our point of interest. Since one of our goals is to keep the antenna height as minimum as possible, the impacts of strip widths (W) on antenna performance parameters are observed first for a fixed number of turns. The terminal impedance of the traditional wire-based helix is around 130 Ω which is not compatible with the impedance of the 50 Ω transmission line, and extra focus on impedance matching is required. It is seen from Fig. 3 that with increasing strip widths 'W' from 5 mm to 15 mm, the reflection coefficient is improved significantly; maximum percentage bandwidth ($S_{11} \leq -10$ dB) of 103% (1.92 GHz to 6 GHz) is achieved for a strip width of 15 mm; and it is only 23% for a strip width of 12 mm [10]. This improvement is only achieved by placing the strip face parallel to the face of the ground plane and certainly eliminates the issue of an external impedance-matching transformer. There is no −10-dB impedance bandwidth achieved when the same strip ($W = 15$ mm) orientation is made vertical (ver.) as shown in Fig. 3.

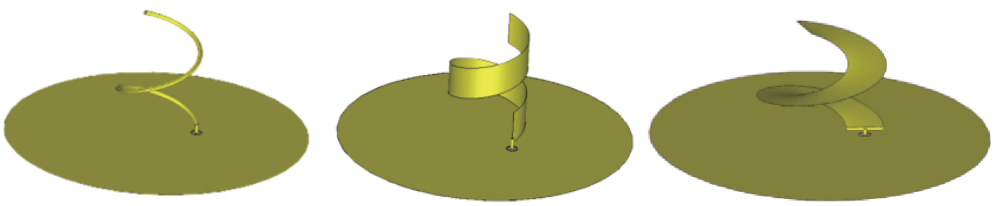

Figure 2. Helical antenna: (a) Wire-based. (b) Strip-based with vertical orientation of the strip face, and (c) Horizontal (non-conformal) orientation of the strip face.

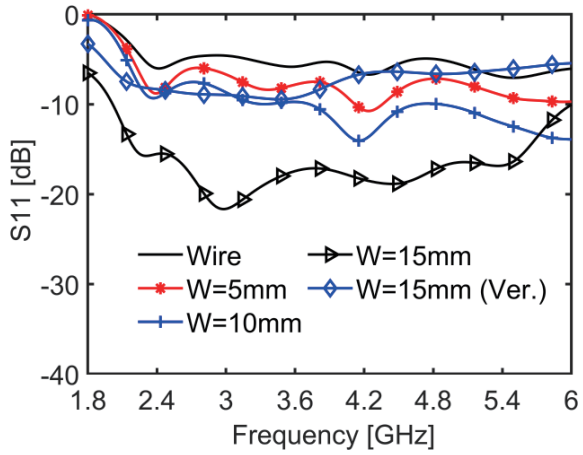

Figure 3. S_{11} comparison with varying strip widths and for vertical strip orientation, when number of turns 1.3.

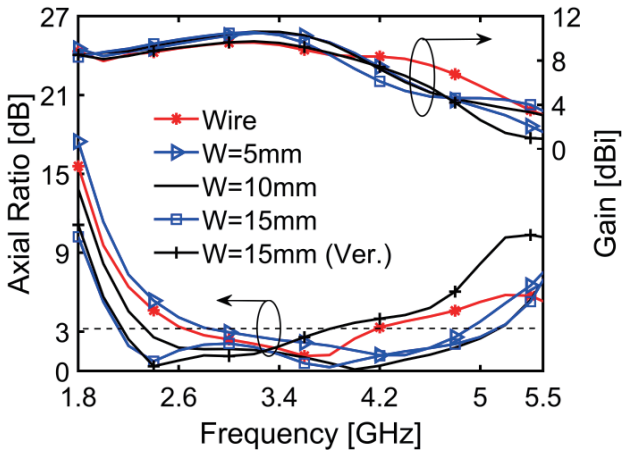

Figure 4. Axial ratio and Gain comparison with strip widths, $N = 1.3$.

The impact of strip widths on AR bandwidth is tremendous and is shown in Fig. 4. The lower frequency of 3-dB AR bandwidth moves toward the left side of the spectrum with increasing strip widths, and as a result AR bandwidth increases. The wire-based helix with the same helix parameters provides the smaller AR bandwidth than any strip width from 5 mm to 15 mm. The maximum 3-dB AR bandwidth of 82.15% (2.13 GHz to 5.10 GHz) is observed for a strip width of 15 mm. Similarly, AR bandwidths of 73.82%, 48.46%, and 41.28% are obtained for strip widths of 10 mm, 5 mm, and wire, respectively. 3-dB AR BW increases 1.7 times from $W = 5$ mm to 15 mm. For the same strip width of 15 mm, the horizontal orientation of the strip provides 1.54 times more AR BW than vertical placement.

Strip widths also have an impact on gain. It is seen from Fig. 4 that up to a certain frequency (3.5 GHz), gain increases with the increase of strip widths as well as with frequencies, and after that, it decreases almost in reverse order and moves toward zero. A strip width of 15 mm provides a gain of 10.55 dBi at 3.2 GHz. On the other hand, individual maximum gains of 10.60 dBi, 10.48 dBi, and 9.62 dBi are provided by strip widths of 10 mm, 5 mm, and wire, respectively. For the same strip width of 15 mm, the vertical placement of the strip provides about 1 dB less gain than the proposed horizontal strip orientation. It is observed that after 3.5 GHz, the main beam deviates significantly from the axial direction which affects gain performance. Up to 3.5 GHz and for $W = 15$ mm, the highest gain variation from the maximum value of 10.55 dBi is 21%.

Next, the number of helical turns (N) is varied by keeping the width of the strip constant ($W = 15$ mm). Changes of 3-dB AR bandwidth with varying N are not uniform, rather abrupt, and are shown in Fig. 5. The maximum 3-dB AR BW of 82.15% (2.13 GHz to 5.10 GHz) is achieved when the number of turns is 1.3 and a minimum of 30% (2.71 GHz to 3.66 GHz) for a single turn. For $N = 2$ and 4, these percentages are 41 and 55, respectively, although the lowest frequency (1.72 GHz) for $N = 4$ in the 3-dB AR band is not shown in Fig. 5. It is needed to mention that the authors in [7] found AR below 3-dB when the number of turns was at least 2.5. In our analysis (not shown), even below a single turn ($N = 0.9$) strip-based helix provides AR below 3-dB although it starts from the right part in the considered frequency band. Gains as usual increase with an increasing number of turns, and maximum gains of 12.45, 11.52, 10.55, and 10.42 (dBi's) are observed for $N = 4$, 2, 1.3, and 1, respectively. Gains sharply fall after 3.4 GHz when the turn number is equal to or above 4. Gain values after 4.2 GHz ($N = 2$) and 3.8 GHz ($N = 4$) are not shown in Fig. 5. The percentage 3-dB AR BWs are very close for $N = 1.3$ and 4, but for maintaining the low profile of the antenna, 1.3 turns strip-based helix is chosen. For designing a helical antenna, recommended pitch angles (α) are in the range of $12^\circ \leq \alpha \leq 14^\circ$. But in this analysis, α is also varied below the suggested values for observing the effects on the strip-based case of a lower number of turns as shown in Fig. 6. A maximum 3-dB AR BW is observed for $\alpha = 14^\circ$. The impacts of pitch angles on gains are not much like AR. From

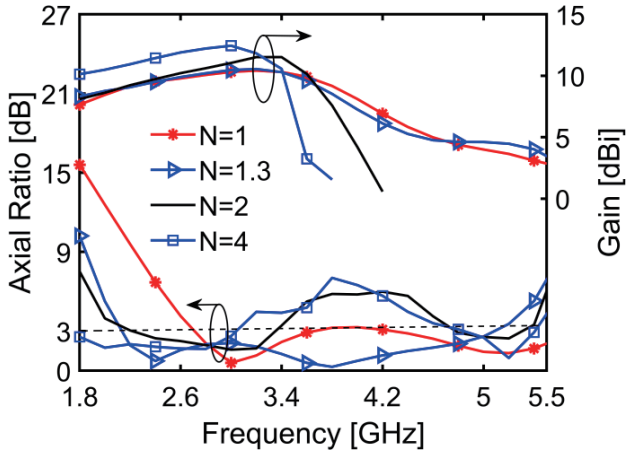

Figure 5. AR and gain with the number of helical turns, when $W = 15$ mm. Gain values below zero (for $N = 2$, 4) are not shown.

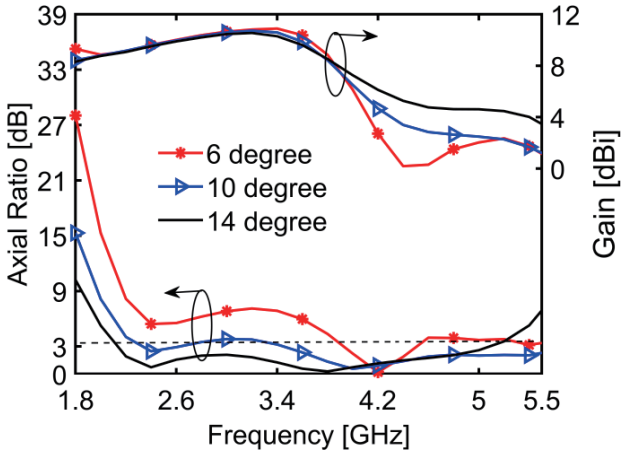

Figure 6. AR and gain variations with pitch angles, when $W = 15$ mm and, $N = 1.3$.

2.8 GHz to 3.6 GHz, gain increases with lower pitch angles without satisfactory values of AR. Based on the above discussion, a strip-based helical antenna of $W = 15$ mm, $N = 1.3$, and $\alpha = 14°$ is chosen for further analysis and simulated with a dielectric-based supportive structure.

3.2. Simulation with Supportive Structure

For ensuring that the fabrication process is rapid and easy, the selected 1.3 turns helical antenna with a strip width of 15 mm is again simulated with a PLA-based supportive structure. The dielectric constant and loss tangent of the material are considered as 3.1 and 0.008, and set these values during the simulation. The width and thickness of the spiral support are 15 mm and 1.5 mm, respectively. Spiral support is attached with five branches originated from the central cylindrical pillar of radius 2 mm. This pillar is also fixed with a circular base (thickness = 1.5 mm) that facilitates making the ground plane. Simulated PLA-based support and that after adding the conducive part on this support are shown in Fig. 7(a) and (b), respectively. The effects of the supportive structure on antenna performance parameters are discussed in this section.

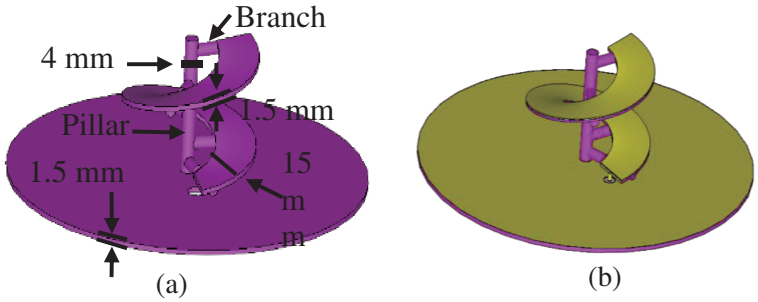

Figure 7. Simulated structures: (a) Only supportive structure, (b) conductive element on the supportive structure.

There is very little effect of supportive structure on impedance bandwidth. It is observed from Fig. 8 that a strip-based helical antenna with a supportive structure provides a −10 dB impedance bandwidth of 97.64% (1.82 GHz to 5.64 GHz) which is only 5% less than a strip-only configuration. There are almost no changes in the 3-dB AR BW and AR values due to the support structure as shown in Fig. 9. Finally, with support, AR $\leq$ 3 dB covers the bandwidth of 82.18%, and it was 82.15% for the

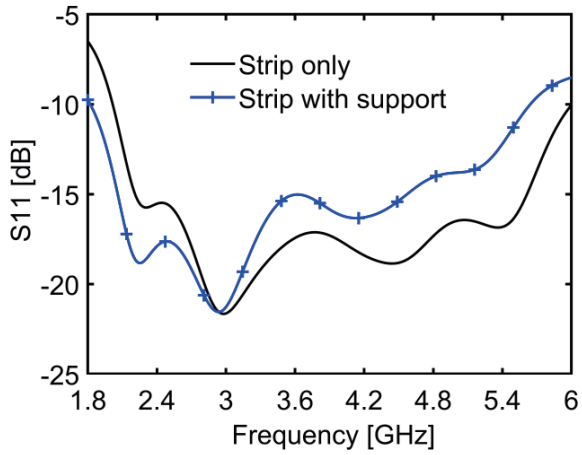

Figure 8. S_{11} comparison between strip and strip with supportive structure, when $W = 15\,\text{mm}$ and $N = 1.3$.

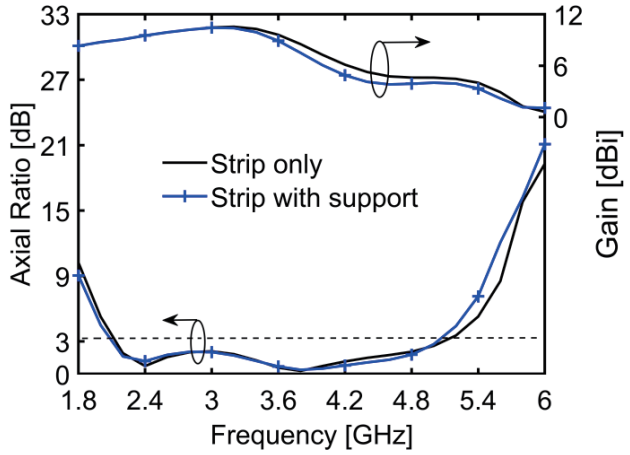

Figure 9. AR and gain comparison between strip and strip with supportive structure, when $W = 15\,\text{mm}$, $N = 1.3$.

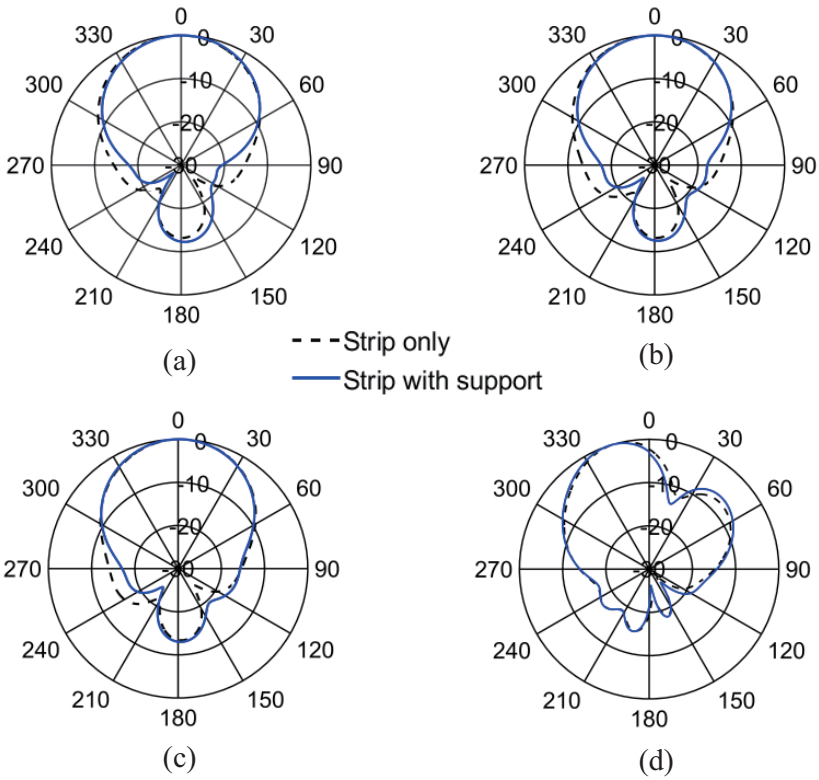

Figure 10. Simulated far-field radiation patterns at $\varphi = 0°$ plane: (a) 2.1 GHz, (b) 2.7 GHz, (c) 3.3 GHz, (d) 3.7 GHz. Polar and radial axes units are expressed in degree (°) and dB respectively.

strip-only case. On the other hand, the same gain performance was observed for both cases of strip-only and strip with supportive structure up to 3 GHz, and after that, there is a maximum 1.24 dBi decrease of gains from the strip-only case.

The impact of supportive structure on radiation patterns is also observed at different frequencies and is shown in Fig. 10. As mentioned before, there is a significant deviation of the main beam from the axial direction, which happens after 3.5 GHz. This deviation of the main beam is possibly due to

the very small number of helical turns. It is also observed that far-field radiation patterns in other planes (not shown) do not change much after adding the dielectric support. 3-dB beam-widths of all considered frequencies agree well. But there is a nominal deviation noticed at 10-dB beam-width due to the supportive structure.

4. CONSTRUCTION AND MEASUREMENTS

The 3D printing process made the construction of this type of complex-shaped antenna easier and faster. After having the supportive structure from 3D printing, copper foil tape is placed over the flat spiral arm as a first approach. The circular ground plane is also ensured by copper tape. As a second approach, silver-coated copper conductive paint is used to create the radiating part and the ground plane. The $50\,\Omega$ flat panel coaxial connector with a straight solder cup is used for external connection (Fig. 11(a)), as well as for measurement. This solder cup-shaped body of the connector allows it to make a nice connection with the ground plane from the upside of the supportive base (Fig. 11(b)). The paint-based ground plane also makes a secure connection by coating the paint on the top of the solder cup (Fig. 11(c)). To make the connection mechanically robust, the flat panel of the connector is glued to the back side of the circular supportive base (Fig. 11(d)). The central lid of the connector is finally soldered with the bottom end of the flat copper strip. No soldering is used for the paint-based approach, and instead, paint is used to make the connection between the end of the central lid and bottom ends of the spiral arm. Pictures of the SMA connector and its attachment with both copper tape and paint are shown in Fig. 11. Finally, the constructed stripped helical antennas using the two approaches are shown in Fig. 12.

(a) (b) (c) (d)

Figure 11. (a) Barrel-shaped connector, (b)–(c) feed points for copper strip and paint-based cases, (d) connector fixed with glue at the back side of the supportive base.

(a) (b) (c)

Figure 12. Photographs of the final fabricated antenna: (a) copper-strip based (b) conductive paint-based (c) antenna in an anechoic chamber.

4.1. Reflection Coefficient (S_{11}) Measurement

S_{11} measurements of the constructed copper strip and conductive paint-based helical antenna are performed by Agilent E8362C Performance Network Analyzer. Fig. 13 shows the measured reflection

coefficient (S_{11}) and is compared with the simulated result. It is seen that for the case of the copper strip, the measured values are well satisfied with $S_{11} \leq -10$ dB throughout the frequency range and maintain good harmony with simulated results. In the case of the paint-based approach, although S_{11} values are not much lower than the case of copper strip and simulated data, it still satisfies $S_{11} \leq -10$ dB. Finally, measured -10 dB impedance bandwidths for copper strip-based and paint-based approaches are 99% (1.86 GHz to 5.5 GHz) and 96% (1.93 GHz to 5.52 GHz), respectively. Compared with simulated results, there are 4% and 7% decreases in S_{11} bandwidth for the cases of copper strip and paint-based approaches, respectively. So, measured S_{11} agree well with the simulation, and the antenna is self-matched, which does not require an additional matching section or transformer.

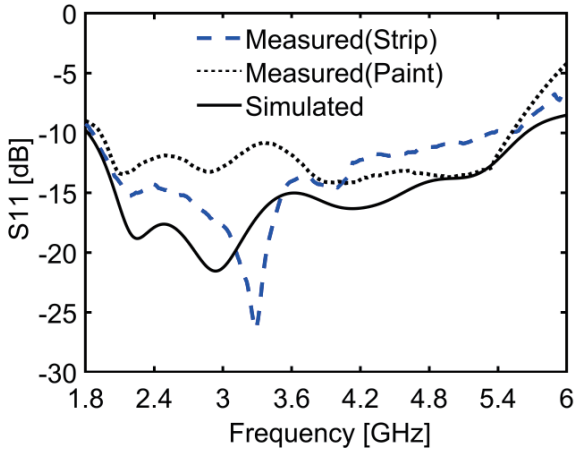

Figure 13. Measured S_{11} of the conductive strip and paint-based helical antenna and compared with simulation.

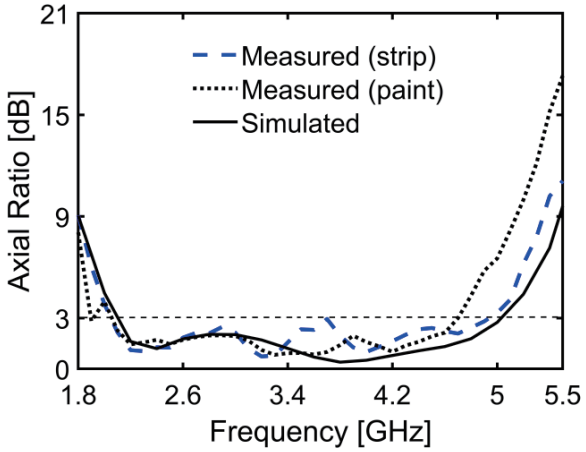

Figure 14. Measured AR of the conductive strip and paint-based helical antenna and compared with simulation.

4.2. Axial Ratio (AR), Gain and Radiation Pattern Measurement

An anechoic chamber with the setup of a Nearfield Antenna Measurement System was used to measure the AR, gain, and radiation pattern of the strip-based helical antenna. A photo of the antenna placement inside the anechoic chamber is shown in Fig. 12(c). From Fig. 14, it is seen that measured AR values for both cases including simulated values have excellent consistency up to 3.1 GHz, and after that,

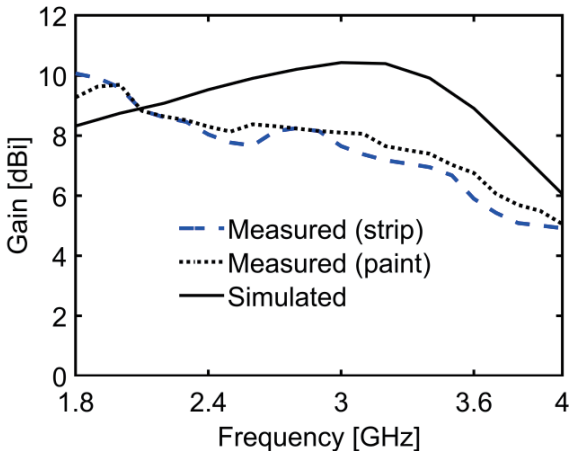

Figure 15. Measured gains of the conductive strip and paint-based helical antenna and compared with simulation.

though AR values are different, they are still $\leq$ 3-dB. Finally, the measured 3-dB AR BWs are 82.52% (2.05 GHz to 4.93 GHz) and 78% (2.07 GHz to 4.70 GHz) for copper strip and paint-based approaches, respectively. For copper strip-based cases, AR BW agrees well with the simulation. On the other hand, in the paint-based approach, there is about a 5% decrease in AR BW from simulation.

The pattern of the measured gains for both cases follows the same way, but magnitudes decrease significantly from the simulated results as shown in Fig. 15. This decrease in the measured gain is due to the more lossy nature of the PLA material at higher frequencies than considered values in simulation. There is a slight improvement of gain for the case of paint, and it is at most 0.68 dBi from the copper strip-based approach.

The simulated and measured far-field radiation patterns for both copper strip and paint-based helical antennas at four different frequencies and in two planes (φ =0°, φ =90°) are shown in Fig. 16. There is almost no difference in radiation patterns between the copper strip and paint-based approaches. Also, very close harmony exists between measured and simulated patterns, though after 3.1 GHz the main beam starts to deviate from the axial direction, and these deviations are below 6° up to 3.5 GHz.

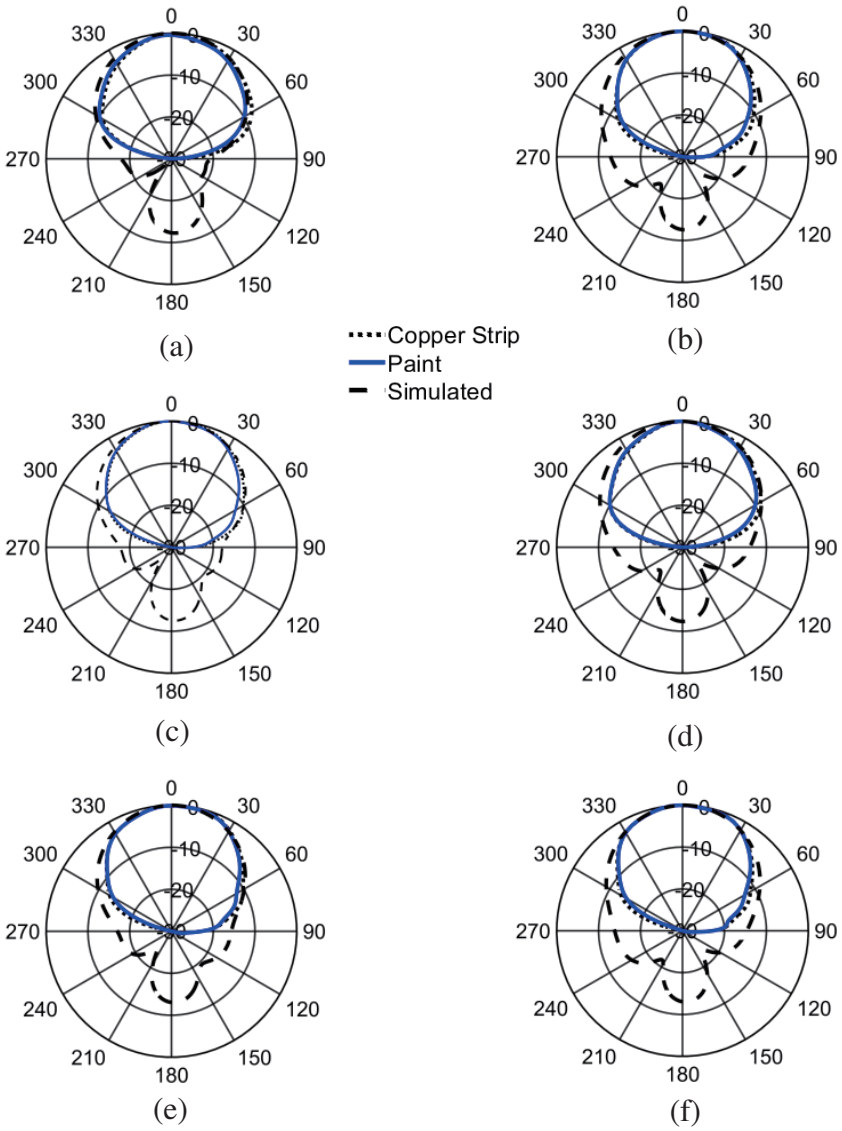

Figure 16. Measured and simulated far-field radiation patterns: (a) 2.1 GHz, $\varphi = 0°$, (b) 2.1 GHz, $\varphi = 90°$, (c) 2.7 GHz, $\varphi = 0°$, (d) 2.7 GHz, $\varphi = 90°$, (e) 3.3 GHz, $\varphi = 0°$, (f) 3.3 GHz, $\varphi = 90°$. Polar and radial axes units are expressed in degree (°) and dB respectively.

Above 3.5 GHz, the main beam not only deviates more but also loses any directionality. Side lobes of the measured patterns below −30 dB are not shown in the polar graphs. In terms of −10 dB beamwidth, there is an improvement in measured radiation patterns for both cases. The measured half-power beamwidth is about 60° which agrees well with simulated results.

The performance comparisons of the proposed strip-based helical antenna with other designs ([4, 9–11, 13, 15]) and their corresponding fabrication approaches are shown in Table 1. AR BW performance of the proposed antenna is at least about 1.5 times of any of the compared designs. Although a similar helical antenna [10] has a bit smaller dimension, it provides about 50% less AR BW than our proposed antenna. Moreover, in their design 44% AR BW was achieved by adding a parasitic patch add the top of the antenna. Mechanically durable support was also an issue there, and it is solved in our proposed technique.

Table 1. Comparison of the proposed antenna.

Ref.	Size (Area) X Height	AR BW (%)	Peak Gain (dBi)	Impedance matching	Supportive material
[4]	$(0.45\lambda_0 \times 0.45\lambda_0) \times 0.28\lambda_0$	24	10	Required	Balsa wood
[9]	$(0.40\lambda_0 \times 0.40\lambda_0) \times 0.52\lambda_0$	46	8	Not required	Hollow dielectric
[10]	$(0.43\lambda_0 \times 0.43\lambda_0) \times 0.25\lambda_0$	44	9.4	Not required	Styrofoam
[11]	$(0.25\lambda_0 \times 0.25\lambda_0) \times 1.12\lambda_0$	54	11.3	Not required	FR4
[13]	$(0.33\lambda_0 \times 0.33\lambda_0) \times 2.70\lambda_0$	31	13.9	Required	Photopolymer
[15]	$(0.32\lambda_0 \times 0.32\lambda_0) \times 0.74\lambda_0$	58	9.8	Required	Nylon
This work	$(0.45\lambda_0 \times 0.45\lambda_0) \times 0.35\lambda_0$	82.52	9.40	Not required	PLA

5. CONCLUSION

A comprehensive analysis of strip-based helical antenna along with different strip orientations and supportive structures is conducted through simulation. By utilizing the advantage of modern 3D printing, the antenna is constructed successfully by using two independent conductive elements. There is very close agreement between measured and simulated results. This low-profile helical antenna provides a wide impedance bandwidth of 99%, 3-dB AR BW of 82.52%, a maximum gain of 9.40 dBi, and a beamwidth of about 60°, and can be used in space communication where smaller size and optimum performance are required. Maintaining almost constant gain throughout the 3-dB AR BW is an issue due to the lossy nature of the used PLA material. Since 3D printing gives the flexibility of construction, additional work on lowering the material density during printing needs to be done in the future to solve the issue. Moreover, depending on specific requirements and applications, a 3D spiral antenna with any arbitrary geometry can be fabricated by utilizing the advantages of additive manufacturing techniques.

REFERENCES

1. Kraus, J., "The helical antenna," *Proceedings of the IRE*, Vol. 37, No. 3, 263–272, 1949.

2. Nakano, H., H. Takeda, T. Honma, H. Mimaki, and J. Yamauchi, "Extremely low profile helix radiating circularly polarized wave," *IEEE Transactions on Antennas and Propagation*, Vol. 39, No. 6, 754–757, 1991.
3. Hui, H. T., K. Y. Chan, and E. K. N. Yung, "The low-profile hemispherical helical antenna with circular polarization radiation over a wide angular range," *IEEE Transactions on Antennas and Propagation*, Vol. 51, No. 6, 1415–1418, 2003.
4. Alsawaha, H. W. and A. Safaai-Jazzi, "Ultrawideband hemispherical helical antennas," *IEEE Transactions on Antenna and Propagation*, Vol. 58, No. 10, 3175–3185, 2010.
5. Chen, Z. and Z. Shen, "Planar helical antenna for circular polarization," *IEEE Transactions on Antennas and Propagation*, Vol. 63, No. 10, 4315–4323, 2015.
6. Sun, W., G. Su, L. Sun, and X. Chen, "A pattern reconfigurable circularly polarized quadrifilar helix antenna through phase control," *IEEE Transactions on Antennas and Propagation*, Vol. 70, No. 9, 7766–7773, 2022.
7. Beneck, R. J., G. Mackertich-Sengerdy, S. Soltani, S. D. Campbell, and D. H. Werner, "A shape generation method for 3D printed antennas with unintuitive geometries," *IEEE Access*, Vol. 10, 91294–91305, 2022.
8. Mirzaee, M. and Y. Kim, "On the far-field characteristics of a 3D-printed antenna using wood-based PLA and conductive silver nanoparticle ink," *United States National Committee of URSI National Radio Science Meeting (USNC-URSI NRSM)*, Denver, 2022.
9. Tang, X., B. Feng, and Y. Long, "The analysis of a wideband strip helical antenna with 1.1 turns," *International Journal of Antennas and Propagation*, Vol. 2016, No. Article ID 5950472, 2016.
10. Tang, X., Y. He, and B. Feng, "Design of a wideband circularly polarized strip helical antenna with parasitic patch," *IEEE Access*, Vol. 4, 7728–7735, 2016.
11. Siahcheshm, A., J. Nourinia, C. Ghobadi, and M. Shokri, "Circularly polarized printed helix antenna for L- and S-bands applications," *Radioengineering*, Vol. 29, No. 1, 2020.
12. Helena, D., A. Ramos, T. Varum, and J. N. Matos, "Antenna design using modern additive manufacturing technology: A review," *IEEE Access*, Vol. 8, 177064–177083, 2020.
13. Ghassemiparvin, B. and G. Nima, "Design, fabrication, and testing of a helical antenna using 3D printing technology," *Microwave and Optical Technology Letters*, Vol. 62, No. 4, 2019.
14. Farooqui, M. F. and A. Shamim, "3-D inkjet-printed helical antenna with integrated lens," *IEEE Antennas and Wireless Propagation Letters*, Vol. 16, 800–803, 2017.
15. Tawk, Y., "A dynamic dual tapered 3-D printed nested helical antenna," *IEEE Transactions on Antennas and Propagation*, Vol. 68, No. 2, 697–702, 2020.
16. Majumdar, B., B. David, C. Sudipta, and E. P. Karu, "Additive manufacturing of a dual-ridged horn antenna," *Progress In Electromagnetics Research Letter*, Vol. 59, 109–114, 2016.
17. Tokan, F., D. Selami, and Ç. Alper, "Influence of 3D printing process parameters on the radiation characteristics of dense dielectric lens antennas," *Progress In Electromagnetics Research C*, Vol. 116, 113–128, 2021.
18. Bjorgaard, J., H. Michael, H. Eric, M. Milad, H. C. Yi, and N. Sima, "Design and fabrication of antennas using 3D printing," *Progress In Electromagnetics Research C*, Vol. 84, 119–134, 2018.
19. Balanis, C. A., *Antenna Theory: Analysis and Design*, NJ, Wiley, 2005.